DOI: 10.13009/EUCASS2019-633

Space Rider Mission Engineering

Davide Bonetti, Gabriele De Zaiacomo*, Gonzalo Blanco Arnao*, Giovanni Medici*, Irene Pontijas Fuentes*, Baltazar Parreira×*

**Deimos Space S.L.U. davide.bonetti@deimos-space.com, Ronda de Poniente 19, 28760 Tres Cantos, Spain*
×Deimos Engenharia, Av. D. Joao II, No.41, 10th floor, 1998-023 Lisboa, Portugal

Abstract

The ESA Space Rider program aims at providing Europe with an affordable, independent, reusable end-to-end integrated space transportation system, for routine access and return from low orbit. It will be used to transport payloads for an array of applications, orbit altitudes and inclinations. The Space Rider is composed of an expendable AVUM Orbital Module (AOM) and of a reusable Reentry Module (RM), which is designed to be flown multiple times. For the RM this translates into the need for a flexible and robust system, able to cope with a wide range of flight conditions, in compliance to stringent safety constraints in case of failure. This is a critical additional challenge for Europe, beyond the current state of the art in re-entry technology represented by the successful flight of the ESA IXV (Intermediate eXperimental Vehicle) on February, 11th, 2015.
This paper presents the current status of the Space Rider Mission and the Mission Engineering results achieved by DEIMOS Space at the System Preliminary Design Review (SPDR). The Mission Engineering is a design process that includes multiple activities in support to the mission and system design: from aerodynamics and flying qualities aspects to End-to-End (de-orbiting to touchdown) reference trajectories optimization, sizing trajectories for subsystems specifications, assessment of the mission performance through Monte Carlo simulation campaigns, and visibility and safety analyses.

1. Introduction

On February, 11th, 2015, the successful flight of the Intermediate eXperimental Vehicle (IXV) allowed demonstrating the European independent capability to return from space. IXV (Figure 2) was a lifting body vehicle with two movable flaps for aerodynamic control that performed a suborbital mission, allowing in-flight demonstration of critical technologies for hypersonic flight conditions and successive re-entry from LEO. After being injected by VEGA in a 400km altitude orbit, IXV performed a successful entry targeting the desired parachutes triggering conditions, to start the final descent for a safe splashdown in the Pacific Ocean.
Leveraging on IXV development, qualification and mission success, intended as an European “intermediate” step toward multiple future space applications, the European Space Agency (ESA) initiated an effort to develop a sustainable reusable European space transportation system integrated with the VEGA C launcher, the Space Rider (SR) currently under development, to enable routine launch and return space missions [1]. VEGA C and the Space Rider constitute an Integrated Space Transportation System (ISTS, Figure 1), composed by:

- Module 1 = the Launch and AVUM Orbital Module (AOM), physically consisting of the Vega C launcher with a specifically adapted AVUM, with the latter acting as orbital service module up to de-orbit boost and separation from the Re-entry Module (RM).
- Module 2 = the Re-entry Module (RM), starting its active role at orbit acquisition, performing the in-orbit payload operations with the AOM support, and remaining active until completion of landing on ground.

The Space Rider RM will have a Multi-Purpose Cargo Bay (MPCB) able to integrate a number of modular payloads to fulfil multiple mission objectives and to perform experimentation of payloads for multiple space applications.
Designed to be an operational demonstrator able to perform at least 5 missions, the Space Rider will have to support orbital operations in multiple orbital scenarios, from SSO to equatorial, deorbit and flight back to Earth with high manoeuvrability and controllability throughout all flight regimes (i.e. hypersonic, supersonic, transonic, subsonic) to perform a safe and precise soft-landing on ground under parafoil. The vehicle is therefore required to have the flexibility to ensure that environmental and operational unexpected events are mitigated and to guarantee the accomplishment of the mission objectives in compliance to stringent safety constraints in case of failure.

DOI: 10.13009/EUCASS2019-633

Figure 1: The Space Rider concept (credits: ESA).

Figure 2: The IXV after the successful re-entry (credits: ESA).

While the heritage from the IXV mission is highly applicable to the mission design for SR, IXV was injected directly by VEGA in a suborbital trajectory, and did not perform an orbital phase nor needed to carry out a deorbit manoeuvre. Also, IXV used a supersonic drogue chute, and hence it did not fly through the transonic regime. Moreover, the SR is an operational vehicle, that will support a range of mission types. Hence SR presents new challenges for the mission design of the coasting and re-entry phase and requires the development of European capabilities to fly the lifting vehicle aeroshape through the transonic regime, which places in particular constraints and challenges on the vehicle's flying qualities during the lower Mach regime from Mach 1.2 to Mach 0.7.
DEIMOS Space is in charge of the Mission Engineering activities, currently at the System PDR, including end-to-end Mission Analysis and Flying Qualities, for the Space Rider, a role that also had in the successful IXV, from the design phase up to launch and flight operations [2].
This paper presents the Mission Engineering activities of the Space Rider vehicle carried out in the phase B of the programme in support to the System Preliminary Design Review (SPDR). The assessment of the orbital scenarios and the definition of the re-entry opportunities were performed, to target the desired landing site within the proposed landing site network. The specification of the optimum Centre of Gravity (CoG) box compatible with the layout capabilities was carried out, in addition to the characterization of the Entry Corridor for trajectory design (focusing in particular on the supersonic and transonic phases not covered by the IXV), the selection of the optimum Angle of Attack (AoA) trim line to be flown, and the associated Flying Qualities performance. End-to-end (de-orbiting to touchdown) optimum reference trajectories were computed, as well as sizing trajectories for subsystems specifications (e.g. TPS, parachutes), and the mission performance were assessed through Monte Carlo simulation campaigns. Finally, the analysis of the visibility of the SR from ground stations during the flight was carried out, as well as the analysis of the telemetry link during the orbital phase, and safety analyses (off-nominal footprints) were executed in order to verify the compliance with the applicable safety requirements.

2. Space Rider Mission and Vehicle Overview

At the beginning of the SR programme, a trade off was carried out to at first select the most appropriate aeroshape class among different classes, and then define the baseline configuration within the selected class [3]. The current baseline design of the Space Rider RM has the same aeroshape and size as the IXV (shown in Figure 4). The SR RM is a lifting body, with no wings, and provides a lift-to-drag ratio of about 0.7 in the hypersonic regime.
With respect to the IXV mission, the SR mission will have to support orbital operations in multiple orbital scenarios, deorbit and re-entry to perform a safe and precise soft-landing on ground under parafoil (Figure 3). In particular:

- The SR ISTS is launched from Kourou onboard the Vega C launcher and injected into orbit.
- During the orbital phase the SR objective is to accomplish the goals for the specific orbital mission. Target orbits currently considered are circular, have an altitude of 400 km, and with an inclination range from equatorial to SSO, depending on the mission objectives.
- At deorbiting, the SR executes a deorbit boost to target the desired conditions at the EIP. After the boost is completed, the RM separates from the AOM and performs a ballistic coasting phase prior to entry. Attitude control during this phase is carried out by means of the Reaction Control System (RCS). The targeted conditions at the EIP are typical of LEO return missions, with co-rotating velocities beyond 7.4 km/s.
- The RM then performs a guided gliding re-entry from the EIP until low supersonic regime (at Mach 1.6), when transition into TAEM phase occurs. The TAEM phase objective is to get the vehicle to the desired conditions (position, velocity, attitude) at the DRS triggering.

DOI: 10.13009/EUCASS2019-633

- At approximately Mach 0.73 the DRS sequence (this terminology was inherited by IXV) is triggered, and a pilot chute, a conical ribbon drogue, and a Disk-Gap-Band drogue are deployed successively to slow the vehicle down toward the desired conditions for the parafoil deployment, that occurs at 6 km of altitude and about Mach 0.12. The parafoil allows to glide with a shallow flight path angle and to manoeuvre to reach the desired landing site.
- The flight terminates with an approach and landing phase at the desired landing site. In this phase the vehicle performs a flare manoeuvre to achieve the proper touchdown conditions.

Multiple orbital mission scenarios have been considered, according to the system needs and specifications provided. The process has been highly dynamic with the main objective of contributing to the feasibility verification of the mission scenarios under investigation from the mission analysis standpoint. Orbital mission analyses were provided to support the orbital mission definition for different orbital scenarios and payloads (e.g. microgravity, Earth observation). Depending on the orbital scenario, different landing sites were considered, and different vehicle configurations are possible. Therefore, the Entry and TAEM phases could vary accordingly. In particular, the re-entry phase will depend on the co-rotating velocity and the FPA at the EIP, the RM mass, and the targeted downrange to be flown during entry. For the SPDR, up to 8 different return mission scenarios (Case 1 to Case 8) have been considered (see Figure 5). Feasible return solutions have been identified for each one of them, including the definition of E2E reference return trajectories from de-orbiting to touchdown. A preliminary verification of the mission performance has been then carried out focusing on the baseline mission design and the backup scenario (Case 1 and Case 3, respectively).

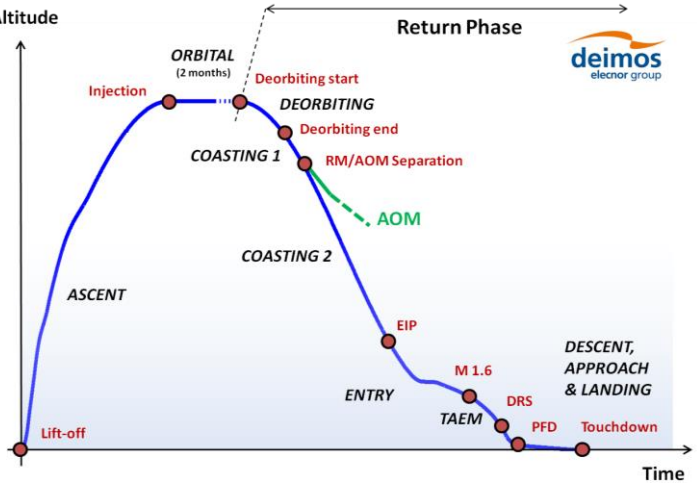

Figure 3: The Space Rider reference mission.

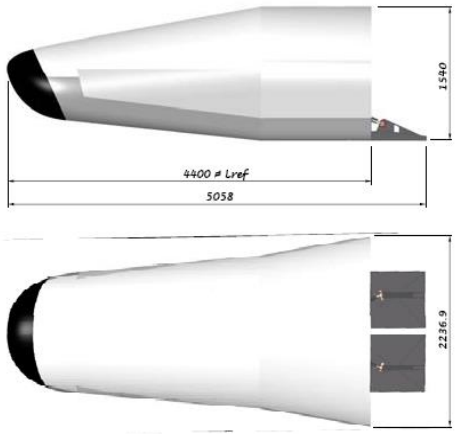

Figure 4: The IXV/SR RM aeroshape (credits: TAS).

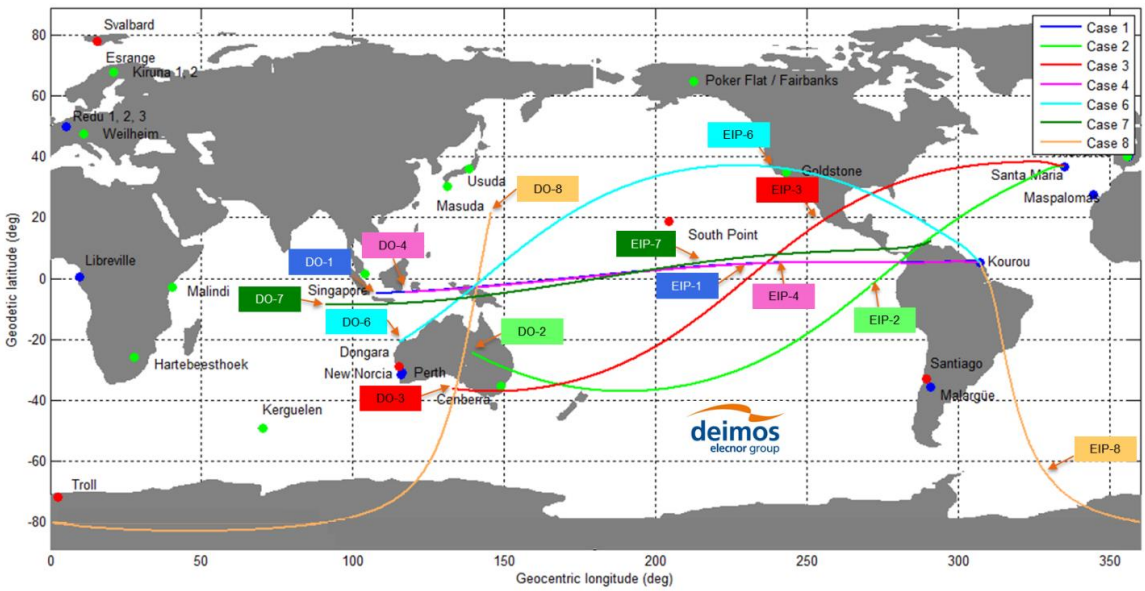

Figure 5: Reference groundtrack of the SR return mission cases (DO: Deorbiting, dots = Ground Stations)

DOI: 10.13009/EUCASS2019-633

3. Orbital Phase Analyses

For the orbital phase, several analyses were performed, covering the range of six different orbital scenarios of interest for the Space Rider missions (Quasi-Equatorial, Medium Inclination, and SSO, with different vehicle attitudes depending of the payload primary mission: e.g. Earth observation or micro-gravity). Results were obtained with on 3DoF and 6DoF simulations which leverage on the orbital aerodynamic database developed by DEIMOS Space for the AOM+RM assembly considering 4 different orientations of the solar panels attached to the AOM (see Figure 6).
The analysis of the environmental perturbations showed that the aerodynamic torques and gravity harmonics accelerations are the dominant effects, while for example the solar radiation pressure has a negligible impact in comparison to the two main contributors. Results supported the sizing of the orbital GNC and to guarantee proper environment for the selected payload applications in orbit.
The Sun direction relative to the SR vehicle was studied for different scenarios and launch dates, showing that there are some orientations where the Sun is not present. This result could support the thermal analyses and the definition of an optimum radiation panel direction for the thermal control of the P/L environment.
Complementary to the environmental perturbations' analysis, 6DoF simulations were performed to evaluate their impact on the attitude stability of SR in open loop. Moreover, worst case scenarios were identified as the sizing cases in terms of the orbit decay assessment. The results (see Figure 8) showed a clear dependency of the orbit decay on the launch epoch, resulting in a higher fuel consumption (~15 kg in year 2025 against ~5 kg in year 2021) when orbit keeping is required (e.g. for Earth observation missions) and a higher orbit altitude loss in case of orbit keeping maneuvers are not applied (55 km against 9 km, respectively) for missions flying during the peak of the solar activity cycle (see Figure 7). As a result, a dedicated analysis for specific payload and launch date should be tailored in order to develop a detailed assessment of the needed requirements regarding the orbit decay. Furthermore, the results of the 6DoF orbital analysis could be useful to support the definition of the orbital GNC needs.

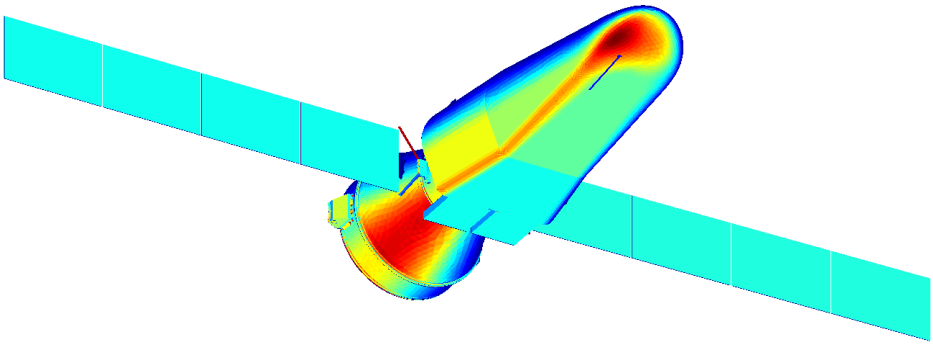

Figure 6: AOM + RM geometry definition and Cp distribution (solar panel rotation = 0 deg)

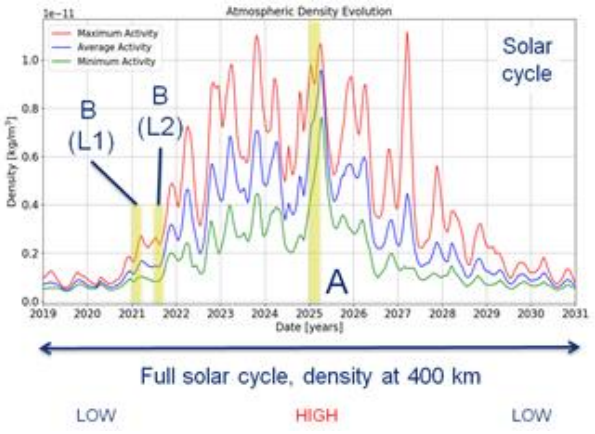

Figure 7: Solar cycle during the epochs considered for the orbital phase mission analysis

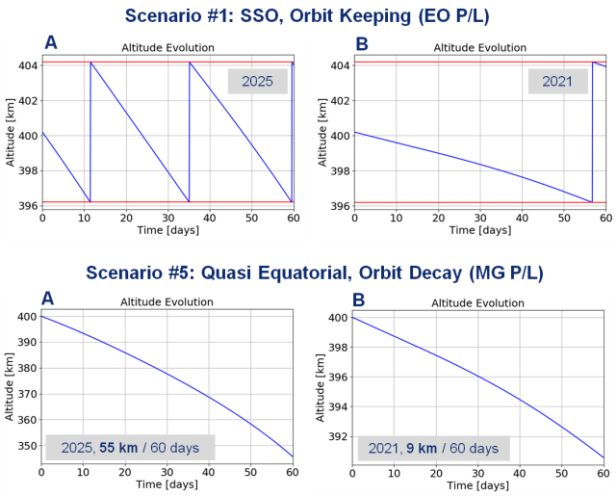

Figure 8: Orbit Keeping and Orbit Decay analyses

DOI: 10.13009/EUCASS2019-633

4. Re-entry Module Configuration Design

In a re-entry vehicle the AoA profile is strongly linked with the mission feasibility and hence its selection and assessment are strictly coupled with the trajectory design. The optimum AoA profile is obtained from an end to end analysis of the vehicle flying qualities and flight mechanics performance in the full range of flight regimes covered by the mission: from rarefied flow, through hypersonic, supersonic and down to subsonic.
The AoA profile (trim line) is the result of a trim process (null moments) where, for a given aerodynamic shape, the vehicle Centre of Gravity (CoG) location play a key role in combination with the aerodynamic surface deflections. Basically, for a given CoG location, an AoA-Mach corridor can be obtained: in this way it is possible to map the feasible CoG locations that are compatible with the applicable constraints and under within the applicable dispersions. In the IXV mission engineering [2], an overall design process was implemented where key vehicle parameters (CoG, AoA profile, Elevators deflections) were coupled through flying qualities (trim, stability and controllability aspects) and detailed mission analysis performance (thermo mechanical loads, landing accuracy, visibility and link budget, safety aspects…) that derived from the trajectory simulation and entry corridor design (where the bank angle profile is also optimized). This approach allows the definition of optimum and robust design solutions guaranteeing feasibility and margins coupling the AoA-Mach corridor (Flying Qualities) with the drag-velocity Entry Corridor (Trajectory Design).
For Space Rider, a similar process was applied, and extended to the transonic and subsonic regimes, not covered by the IXV. Additionally, another degree of freedom was added to the problem, that is the variability of the aeroshape. At the beginning of the study, in phase A, a trade-off on the candidate aeroshape classes was carried out [3], resulting in the selection of the Lifting Body as baseline aeroshape class. Within the Lifting Body class, two options were analyzed: the IXV aeroshape, and the IXV aeroshape with fins. On one side, the IXV aeroshape maximized the IXV heritage from any perspective and ensured the extension of fly-ability envelope down to transonic and subsonic regimes. On the other, the IXV with fins was a promising variant especially in terms of maximization of the vehicle flight capability, and lateral-directional static and dynamic stability, even if with significant drawbacks in terms of mass increase, structural modifications and an additional effort for the characterization of the aerodynamics and aero-thermodynamics properties. In this context, Flying Qualities (FQs) analyses were carried out to support the trade between the two solutions. The results confirmed the possibility to cross the transonic/subsonic regimes with the IXV configuration, that was the selected as the baseline solution for the Space Rider Preliminary design [4].
Once the configuration was selected, Feasible Domain (FD) analyses were carried out to support system trade-offs decision on the vehicle configuration design, in particular in the selection of a robust nominal CoG location that results into satisfactory FQ Entry Corridor performance (margins with respect to FQ constraints). An analysis much wider and detailed than in IXV (see Figure 9) was carried out. Overall, about 1.7 million Monte Carlo shots were processed. Results show that the entry corridor shrinks in the subsonic regime, due to limits in trim constraints.

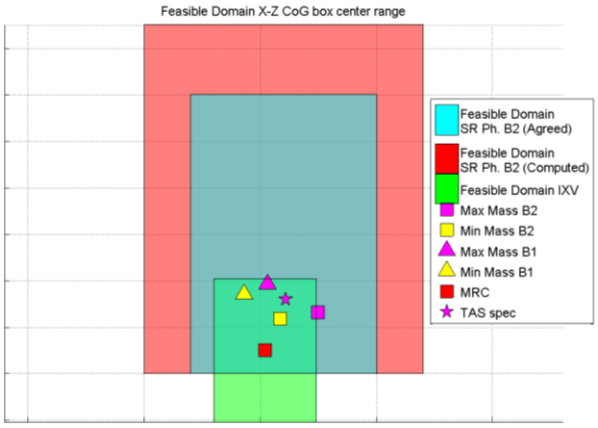

Figure 9: CoG X-Z box comparison, SR vs IXV

While the IXV entry finished at Mach 1.5 (where the corridor was more than 10º width), in Space Rider the objective is to fly the challenging transonic phase and the corridor is less than 5º below Mach 0.85. Depending on the set of constraints, and on the flap range available for trim, CoGs for which the Entry Corridors opens up down to Mach 0.6 could be identified (see Figure 10). In general, the CoG range explored allows playing with about 1º of Entry Corridor width at the same Mach (in the region of Mach < 0.85). Punctual issues around Mach 0.82 exist for a subset of the CoG. Overall, the IXV CoG is confirmed to be a feasible solution, even if it is not the numerical optimum at FD level. Other CoGs offer better performance, in particular at Mach 0.73 (nominal DRS) cases with 2º corridor width exist (vs 1º for IXV CoG), and the most promising region to be investigated at system level for the design of the vehicle CoG were identified.
The software used to perform all the Flying Qualities analyses is the DEIMOS Space S.L.U. FQA Analysis Tool that has also been extensively used in multiple projects of the European Space Agency [5]. More details and results of both FQs and trajectory design are presented in the next sections.

DOI: 10.13009/EUCASS2019-633

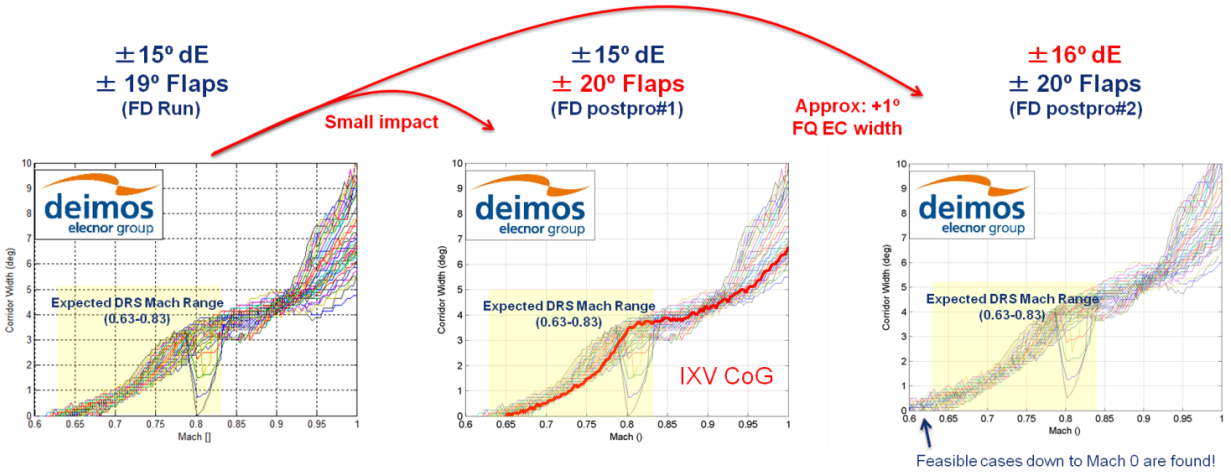

Figure 10: Corridor width as a function of Mach

5. Flying Qualities

The vehicle configuration design (the aeroshape definition, CoG location and trim line design solution) is provided as an input for the Mission and GNC design disciplines. Flying Qualities (FQ) are evaluated with dedicated Monte Carlo functionalities of the FQA Tool in order to characterize the trim, stability, and control characteristics, and margins as input to GNC activities.

For the baseline configuration selected, a trim line design solution was identified within the available entry corridor: the IXV solution for the hypersonic and supersonic regimes was confirmed for the Space Rider, and a feasible trim line was designed for the low supersonic, transonic and supersonic phase (Figure 11).

Results presented in this section are based on a Monte Carlo campaign of 4000 shots including uncertainties on aerodynamics, AoA tracking, inertia properties, dynamic pressure, CoG location and GNC allocation in all flight regimes. The evaluated FQs comprise trim characteristics, static and dynamic stability, dynamic couplings, spin tendency, and hinge moment needs. FQ verification showed good performances in hypersonic as long as a trim is achievable with aerodynamic means (dynamic pressure > 250 Pa), with a slightly undamped Dutch Roll, yet with a considerable time to double and therefore no possibility to develop during the entry phase. In supersonic/transonic, no instability is found in lateral-directional. In supersonic, in terms of longitudinal stability, all cases are stable, while during the transonic regime only 1 case (out of 4000) is unstable between Mach 1.12-1.14, with a minimum time to double of 1.35 s. On the other hand, the IXV trim approach (i.e. to make use of the aerodynamic surfaces to trim the vehicle) shows a more important instability in the subsonic regime below Mach 0.8-0.9 although with a higher time to double (about 50 seconds) which indicates that the development of the instability is not likely to occur.

Nevertheless, an alternative approach was investigated: to command a fixed elevon vs Mach profile, while the vehicle is allowed to "free fly" (i.e. AoA is let free for trim with the aileron and the sideslip angle). This solution is valid from a FQ perspective and it basically leverage on the high pitch stability of the vehicle in transonic/subsonic. The drawback of this “de trim” approach is a wider variability in the AoA that is obtained against a closed loop control strategy, that have an impact on the trajectory (a dispersion in AoA leads to a dispersion in L/D and therefore on the range controllability during free flight) and on the Descent sub-system (a wide dispersion on AoA could become a challenging requirement for the drogue parachute design).The results obtained showed that the AoA variability is around 10º from Mach 0.9 to Mach 0.6. with a positive static longitudinal stability throughout all the trimline. If this strategy is implemented, all cases are stable below Mach 0.9. Figure 13 shows, for example, the 99% range of variability (blue: lower limit; red: upper limit) with 90% confidence level for the AoA, the trim elevon deflection, and the static margin SM. The static margin is defined as the distance between the actual CoG and the position of the centre of gravity at which stability is neutral (neutral point), and is a static stability indicator. Levels of SM above zero are considered satisfactory. The results of the campaign verify and validate that an optimal and robust solution has been designed for the current configuration achieving good overall performances with margins. With the IXV trim approach. the AoA corridor is verified and good performances are validated down to Mach 0.9, with no saturations on the control surfaces, acceptable sideslip variability and no relevant dynamic instabilities. Below Mach 0.9, the "de trim" approach is proposed, with very good performance in terms of stability and controllability. The supersonic, transonic and subsonic FQs have been validated afterwards with the results of the 6 DoF GNC Monte Carlo for the Entry and TAEM phase [7], in particular the trim performance. The variability from the FQ results properly predicts the variability obtained with the GNC (Figure 12 shows for example the angle of sideslip), and the margins assumed in the FQ analyses are appropriate.

DOI: 10.13009/EUCASS2019-633

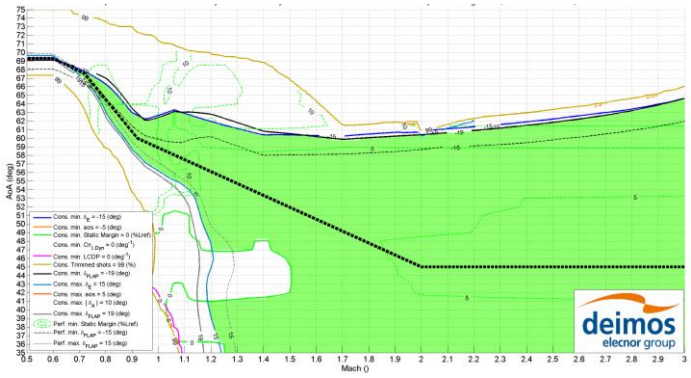

Figure 11: Trimline solution for Space Rider in supersonic/transonic regimes

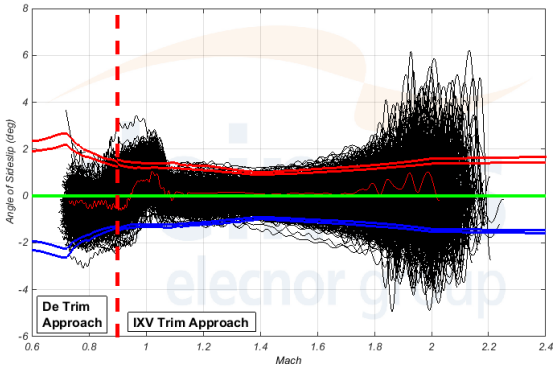

Figure 12: Validation of FQ prediction with 6DoF GNC results

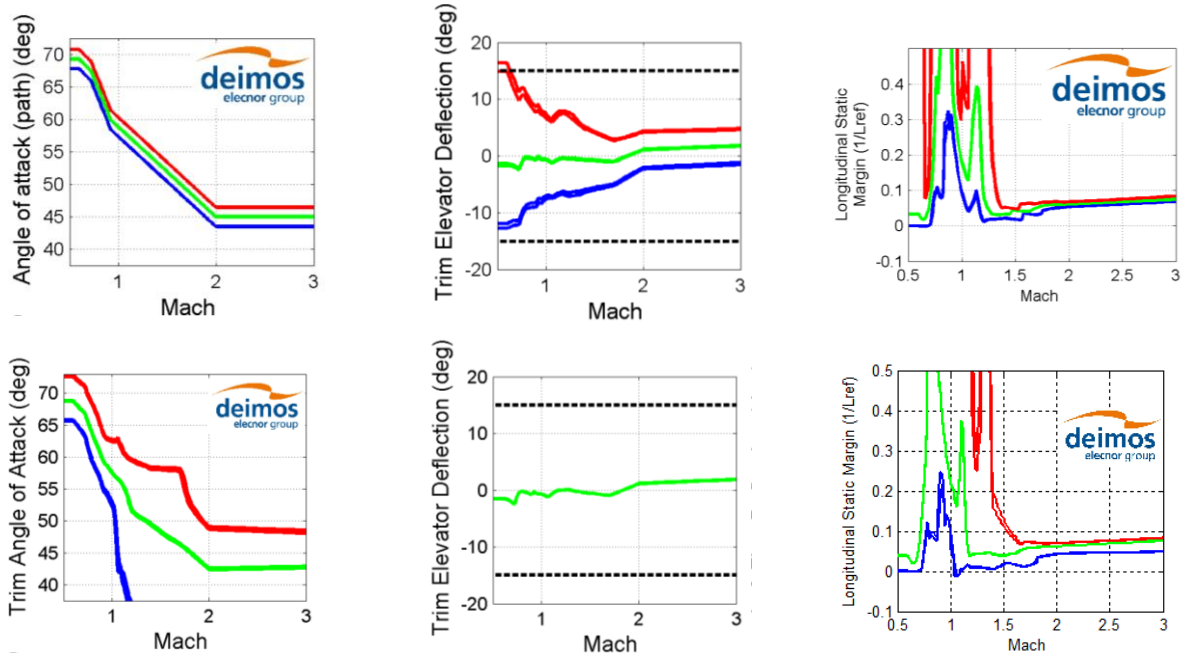

Figure 13: AoA. elevon deflection, and static margin variability, IXV trim (up) vs “de trim” strategy (down)

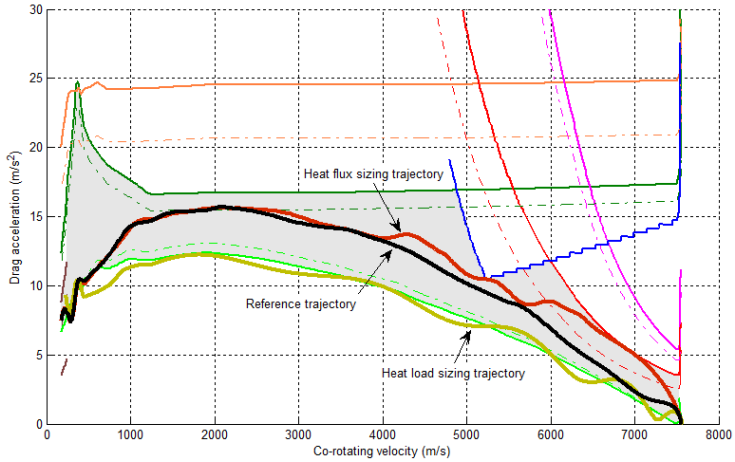

Figure 14: Reference and sizing trajectories w.r.t. Entry Corridor

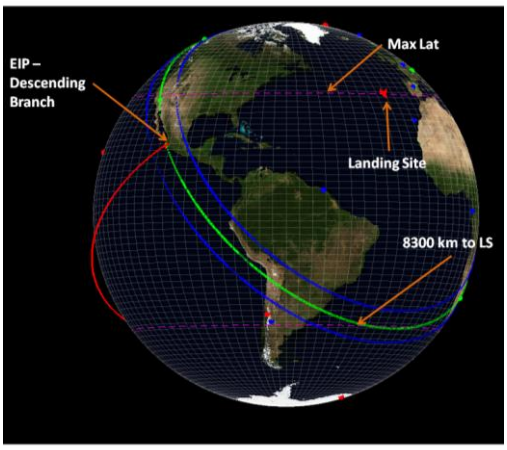

Figure 15: EIP targeting for Azores

DOI: 10.13009/EUCASS2019-633

6. End-to-End Trajectory Design

The trajectory design is a multiphase problem where the definition of the reference mission needs to be compatible with all of the Mission and System constraints with adequate margins for GNC operations. The considered constraints include the deorbit opportunities from the operative orbit to the desired landing site within the landing site network, vehicle thermo-mechanical limits during entry, stability and controllability through the trim line design during hypersonic/supersonic/transonic and subsonic regimes, DRS activation limits and descent system operative envelopes, safety restrictions to the Entry Interface Point (failure footprint) and for the final approach toward the landing site, mass margin policy, and visibility from ground stations.

For a given scenario and vehicle configuration, the entry corridor is defined as the flight domain where the vehicle can fly being compliant with the imposed constraints (Figure 14), whose limits are defined by a combination of technology capability (the technology behind each subsystem defines the design limits), System limitations (it can be decided at System level to limit a subsystem below its capabilities in order to avoid oversizing of the vehicle) and mission boundaries (a ceiling limit is designed to ensure no skip-out and return into orbit in case of shallow returns) and are never to be exceeded. Within the Entry Corridor, the sizing trajectories are trajectories that activate the constraint that defines the corridor, and are used for the design of a particular system/subsystem that activates a particular constraint. For the Space Rider, sizing trajectories for the heat flux and heat load were computed to support the design of the Thermal Protection System (see Figure 14), for the maximum mass configuration.

Once the Entry Corridor is defined, the reference trajectory is computed. The computation of the reference trajectory requires a single end to end optimization process from deorbiting to the triggering of the Descent and Recovery System (DRS). The objective of the optimized deorbiting and coasting maneuver is to target the desired conditions (position, velocity and attitude) at the beginning of the entry phase (at the Entry Interface Point, EIP). These conditions have to be compatible with the Entry Corridor limits and with the range capability to reach the desired landing site (see Figure 15). The objective of the entry phase optimization is to calculate an optimum reference trajectory from the EIP to the targeted DRS conditions, compliant with all the entry constraints and assuring maximum margins for the GNC during the entry of the vehicle. The entry optimization is a Full Optimal Control Problem that involves several parameters and control profiles. The software used is based on the DEIMOS Space S.L.U. Sequential Gradient Restoration Algorithm (SGRA) [6]. SGRA is an indirect full optimal control algorithm that allows the optimization of a control profile along with a determined set of parameters having an effect on the problem under study. Specifically, the optimization code developed for IXV [2] was adapted for the Space Rider.

Feasible and optimum end-to-end trajectories were computed for the 8 return scenarios considered (see Figure 5), providing margins for the GNC operations within the entry corridor and being compatible with the orbital phases, the descent system operative envelope and the targeted landing sites. The 8 scenarios include return missions from 5.3 deg (Quasi-Equatorial), 37 deg (Medium Inclination) and 97 deg (SSO) orbits, with the RM mass range between 2028 and 2734 kg depending on the vehicle configuration and the orbital mission scenario, and landing to Kourou, Curaçao, or Santa Maria (Azores). The variability of the velocity at the EIP, coupled with the wide mass range and the need to fly a given downrange during the entry to assure enough trajectory controllability, forced to target in some cases a shallower entry than for IXV (-1.17 deg vs -1.21 deg). Thermal constrains at the vehicle nose and at the flaps, including passive to active oxidation limit for C-SiC Thermal Protection System (TPS) material and transition to turbulence, are respected in all cases with margins, as well as the conditions for DRS triggering (see Figure 16).

Preliminary trajectory solutions were computed for the descent under parafoil phase. For this phase of the flight, the trajectory geometry definition depends strongly on the guidance strategy implemented, and the glide performance vary with respect to the parafoil aerodynamic capability, wind loading, and atmospheric density.

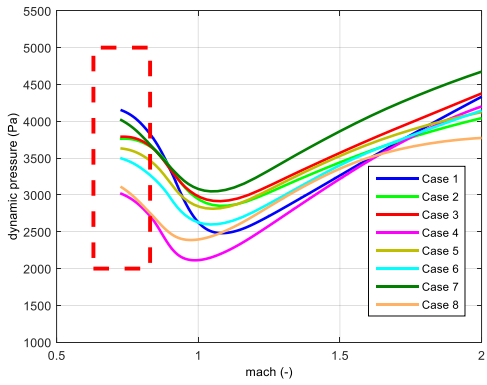

Figure 16: Dynamic pressure vs Mach at DRS

The wind profile has also a profound impact on the trajectory, because the wind velocity may be comparable to the airspeed. In order to guarantee enough margin for trajectory control, the maneuvering energy should be preserved as long as possible. For a constant glide flight, the maneuvering energy corresponds to altitude. A design approach based on a Parafoil Target Area (PTA) analysis was developed in DEIMOS to design a safe and reliable DRS point and Descent trajectory, taking into account the effect on the parafoil flight capability (defined through the equivalent altitude margin) due to System mass, parafoil aerodynamics, and the winds variability in the region of interest (extracted from the NOAA database); any safety constraint (e.g. no fly zones) in case of failures occurring during the Descent phase, and expected accuracy from the GNC (Figure 17). Preliminary trajectories were therefore computed for all the 8 scenarios considered (Figure 18).

DOI: 10.13009/EUCASS2019-633

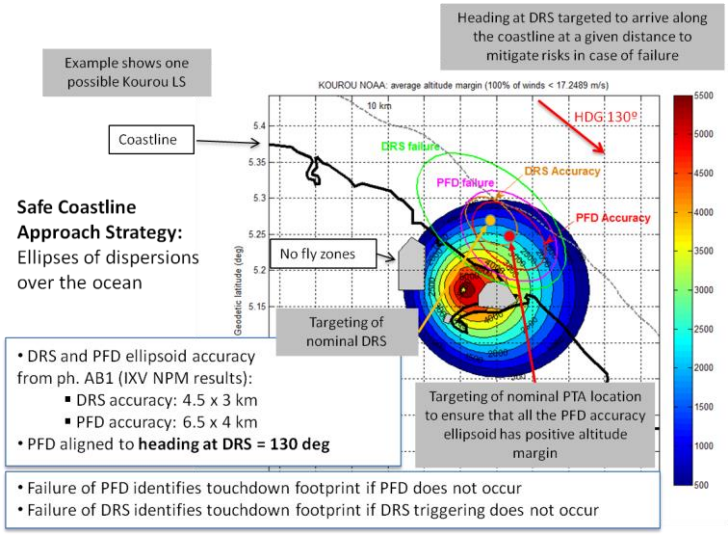

Figure 17: Example of the PTA analyses and PFD optimization for Kourou, highlighting the main aspects of the Safe Coastline Approach Strategy

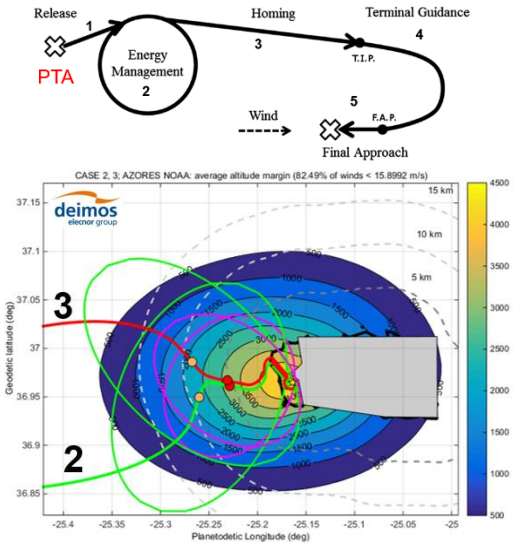

Figure 18: Parafoil descent strategy (up) and reference descent trajectories for scenarios 2 and 3 landing at Santa Maria

7. Mission Performance

The performance and robustness of the mission were preliminary verified using a full simulation from deorbiting to parafoil deployment in the baseline mission scenario. End-to-End Monte Carlo campaign of 1000 shots have been simulated for the baseline (Case 1: QE orbit, maximum mass, Kourou) and backup (Case 3: MI orbit, maximum mass, Santa Maria) scenarios. It comprises the coasting of the RM from the AOM-RM separation until the Entry Interface Point, the guided entry and TAEM phase, and the descent under the pilot, subsonic conical ribbon and Disk-Gap-Band parachutes. These simulations included a proto-Guidance in close loop derived from the Entry and TAEM phases Space Rider Guidance [7], and Navigation and Control performance models inherited from IXV [2][8]. Simulations have been conducted considering uncertainties in the orbital parameters at separation, environment, and vehicle characteristics (mass properties, aerodynamics).

The dispersions at the EIP strongly depend on the accuracy of the deorbit maneuver. At separation the same performance as per IXV were considered, in order to be conservative (thanks to orbit determination and optimization of the de-orbit maneuver the dispersions at SEP are expected to be lower than for IXV), obtaining dispersions at the EIP in line with those considered for the IXV qualification (see Figure 19).

The entry proto-Guidance is able to compensate the large dispersions at the EIP and achieve performance at approximately Mach 1.6 slightly higher than the IXV (6 km vs 5 km obtained by IXV). On the contrary, at the end of the re-entry phase the heading angle is quite different from the reference value ([80 to 105] deg 99% range VS a reference value of 104 deg, see Figure 20). This result is expected because the IXV guidance did not track precisely the heading angle: in the IXV mission there were no requirements on the heading value at the DRS, neither on the heading dispersion. On the contrary, in order to guarantee a safe landing, the Space Rider needs to fly a very precise heading profile in order to implement the safe coastline approach strategy. For this reason, it was suggested to include heading performance requirements based on applicable safety requirements for the entry and TAEM GNC in order to assure that any particular maneuver designed to fly a trajectory respectful of the safety constraint is correctly tracked. During entry, the constraints are fulfilled, in particular ATD, while a violation of the dynamic pressure occurs toward the end of the Entry phase, for the baseline scenario (see Figure 22). The analysis of these results points to a connection with the poor behavior of the proto-Guidance toward the end of the Entry phase.

The TAEM proto-Guidance controls the trajectory during the supersonic and transonic phase and targets the desired heading dispersion to guarantee a precise alignment of the trajectory toward the reference DRS conditions (Figure 23). The pilot triggering is estimated to occur within the DRS box and the in the descent phase the system flies mainly within the parachutes operative envelopes (Figure 21). Performance are indicating that iterations at system levels are necessary to converge to a Descent design compatible with specifications that can be derived from these analyses. This is considered as normal work in next design loops. Position accuracy at the targeted parafoil deployment at approximately 6 km of altitude is lower than 9 km, well within the capabilities of the current parafoil solution (see Figure 24).

DOI: 10.13009/EUCASS2019-633

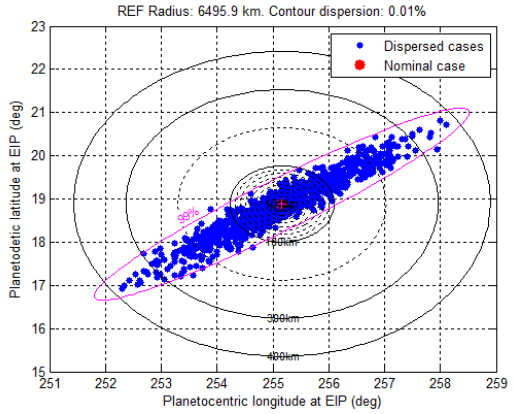

Figure 19: Position accuracy at the EIP (Case 3)

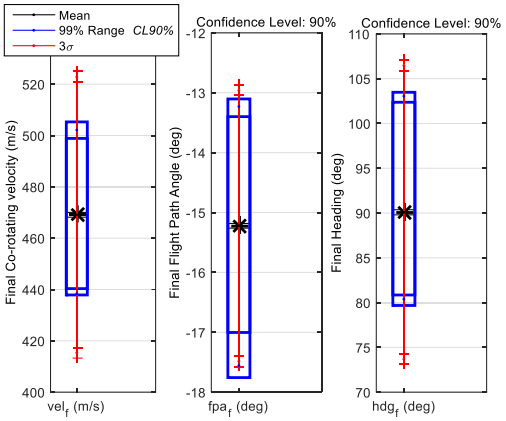

Figure 20: Velocity variability at the end of Entry (Case 1)

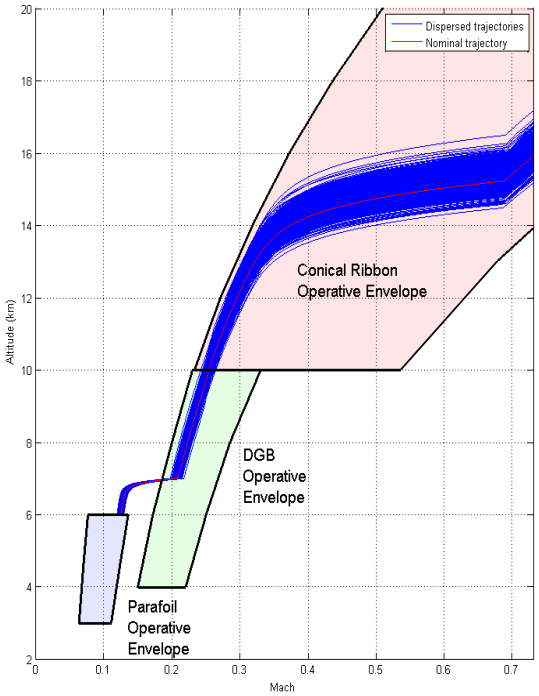

Figure 21: Dispersed descent trajectories (Case 1)

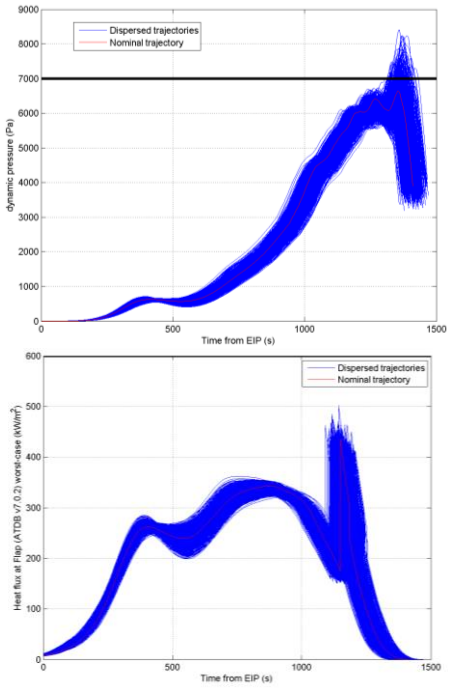

Figure 22: Heat flux at flap and dynamic pressure performance (Case 1)

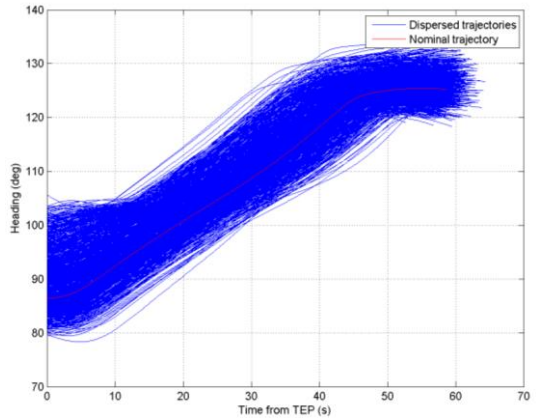

Figure 23: Co-rotating heading angle vs time during the TAEM phase (Case 1)

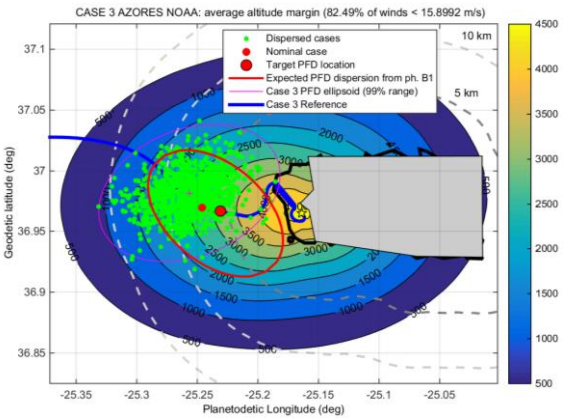

Figure 24: Position accuracy at targeted parafoil deployment condition (Case 3)

DOI: 10.13009/EUCASS2019-633

8. Safety Analyses

In addition to the footprint for the nominal scenario, the corresponding non-nominal footprint in case of a failure of the Space Rider during the return phases was assessed in order to verify the compliance with the applicable safety requirements. Specific analyses and simulations have been run with the objective of supporting the assessment of casualty risk in case of failures, in particular:

- the RM suffering a GNC failure during aerodynamic flight during the Coasting-Entry-TAEM phases leading to an uncontrolled turn and impacting the vehicle as a single object.
- the RM suffering failures at DRS deployment, parafoil deployment, or a parafoil GNC failure (parafoil cut) during the Descent phase leading to an uncontrolled flight and impacting the vehicle as a single object.

For the first set of failures, at first a preliminary analysis of the casualty risk covering the 8 return mission cases and both re-entry dates, 2021 and 2025, has been preliminary derived by combining the results of the IXV safety footprint [2] with the Space Rider range capability, in line with the safety/risks assessment approach used for the phase A/B1 [4]. The analysis was performed considering the Gridded Population of the World Model v4.0 (GPW4 [9]), extrapolated to the targeted date of the mission (2020). The estimated footprints are shown in Figure 25. The worst case in terms of total casualty probability on ground is for the baseline scenario with a return to Kourou (case 1), with an estimation of 1.93E-04 for the year 2025, with over 99% of the casualty risk contributed by the South America region, despite its lower population density w.r.t., for example, Central America. If the probability that this event occurs is set to 1% (as per Space Shuttle Orbiter [11]), the casualty is estimated to be 1.93E-06, compatible with the safety requirements.

Then, a consolidated casualty risk analysis was carried out, by analyzing a complete GNC loss occurring in any moment of the flight between the separation of the RM from the AOM and the DRS triggering. A Monte Carlo campaign of more than 365.000 shots was run based on free 6-DoF propagation of the RM with the failure (initial condition) occurring at any moment of any of the nominal scenario Monte Carlo trajectories. Touchdown conditions were computed, and the final footprint calculated (see Figure 26). Results show that the casualty risk obtained with the preliminary analysis are conservative, while with a more detailed analysis, the casualty risk figure reduces considerably. This second approach is suggested as the new applicable one for the estimation of the statistical footprint in next phases.

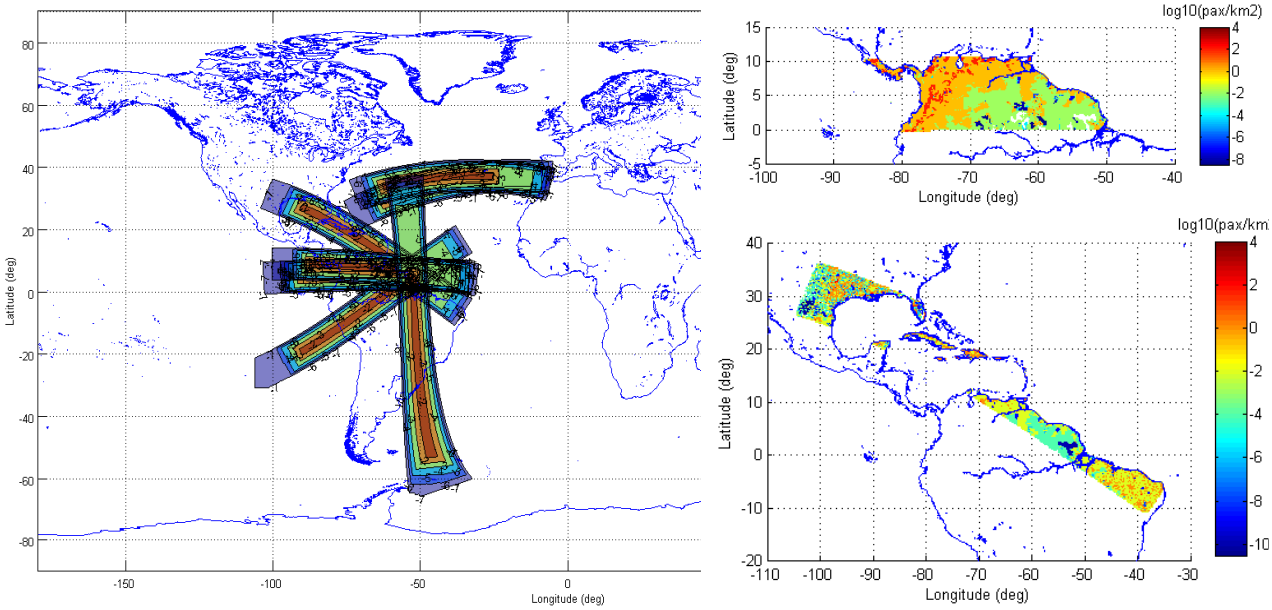

Figure 25: Footprints for the 8 mission scenarios (left), and example of population density distribution for the scenarios Case 1 and Case 6 (right)

DOI: 10.13009/EUCASS2019-633

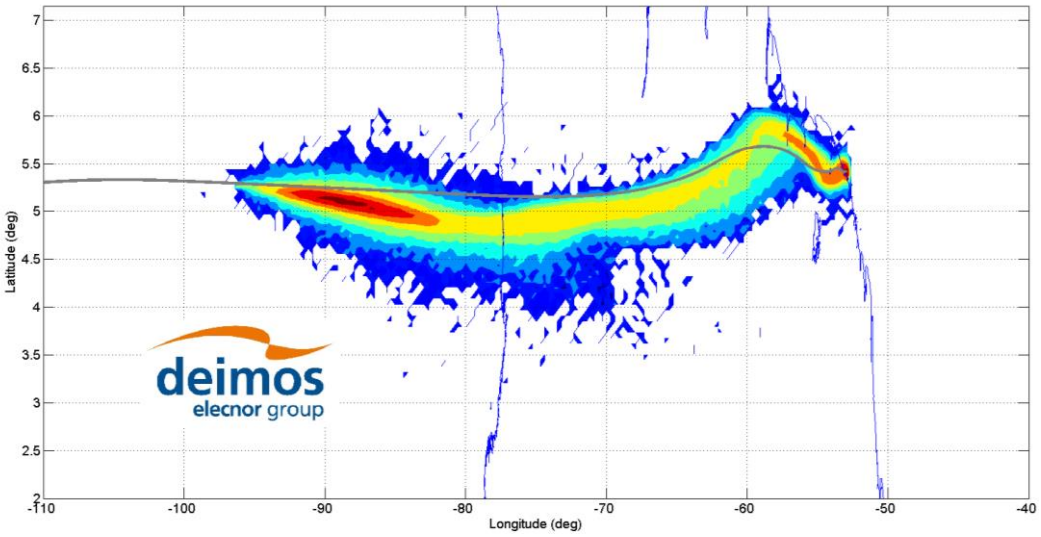

Figure 26: Impact point heat map (log 10 scale) for Case 1. Nominal trajectory is added as a reference for the mission main track

For the failures occurring during the Descent phase, the objective of the analysis was to estimate the casualty risk associated but also to verify the hypothesis in safety considered for the PTA analysis (see section 6). DRS triggering, parafoil deployment, and parafoil GNC failures were simulated, for each dispersed trajectory considered in the Monte Carlo campaigns, assuming an uncontrolled flight from failure event until touchdown. It is remarked that no filtering of the local winds profiles has been carried out (i.e. winds are sampled within the NOAA derive model without checking is the considered wind is compatible with the airspeed of the vehicle; in other words, winds that would have been NO-GO for landing are still considered, very likely leading to conservative results).

Figure 27 shows, for example, the results obtained for a DRS failure for the Case 3 scenario. The footprint of the touchdown location is over the ocean, and well within the footprint assumed for the PTA analysis (99% ellipsoid, [5.6 x 8] km semi-major axis). The associated casualty risk is therefore 0. Similar results have been obtained for the other failures, and for both the baseline and backup scenarios.

Therefore, no casualty risk is associated to the descent phase, and the safety assessment confirmed that the safety margins assumed for the PTA analysis to take into account a DRS failure are conservative.

Furthermore, these analyses confirm that the Safe Coastline Approach defined for the design of the reference trajectories is correct.

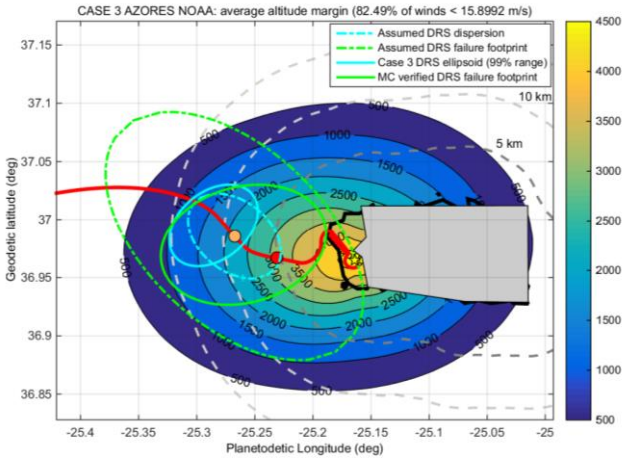

Figure 27: DRS failure safety assessment, Case 3

9. Visibility Analyses

The first objective of the visibility analysis is to evaluate the existence of a line of sight between the Space Rider and a given station of the Ground Station Network (GSN) considering the station antenna mask and SR antennae pattern, in order to evaluate the capability to download to the network of ground stations the telemetry, and with the objective of maximize visibility during the critical events of the mission. The second one, is to carry out the analysis of the telemetry link during orbital phase through the evaluation of the link budget, aiming to assess if a feasible communication link is possible between SR and the ground stations.

A preliminary geometric visibility analysis has been performed for the 8 mission scenarios considered from deorbiting to landing, considering the preliminary baseline GSN solution (Core ESA network, Cooperative network, Augmented network, represented by the green, blue and red points respectively in Figure 5) and different ground stations masks (elevation > 5º or elevation > 0º). Additionally, an Orbital phase starting 2 months (60 days) before the deorbiting is considered for each scenario.

DOI: 10.13009/EUCASS2019-633

Table 1: Preliminary GSN identified for maximum visibility time during the Space Rider Orbital phase

Orbital scenarios	GSN
Quasi-Equatorial (5.3º, 8.7º)	Libreville, Singapore, Malindi, Kourou
Medium Inclination (37º)	Hartebeesthoek, Maspalomas, Dongara, Masuda, New Norcia, Perth, Santiago
SSO (97º)	Svalbard. Troll, Esrange

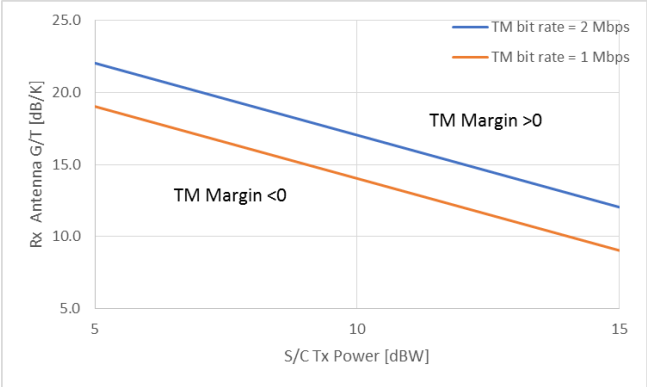

Figure 28: Link budget sensitivity analysis for 5 deg elevation

For the orbital phase, a subset of best stations was identified for each scenario (see Table 1). Multiple contacts per day are observed for all the stations listed above in the cases indicated. It is remarked that no overlap of best stations is observed. The results provided are inputs to the system decision on the network of Ground Station to be considered in the next phases of the Space Rider programme. If larger fractions of coverage are needed, satellite data relay or movable stations in strategic points could be considered.

Following the Space Rider during the return mission, with continuous visibility from ground stations, results to be extremely challenging. In general, contact is lost after the deorbiting maneuver, and recovered in general during the final part of the Entry from the GS available at the landing sites (Kourou and Santa Maria). It is remarked that in Case 7, a mobile station in Curaçao is needed, since no ground station is currently available. In all the other cases, the end of TAEM phase and almost all of the descent phase are visible as part of a final visibility interval lasting more than 20 minutes. The results provided are inputs to the system decision on the network of Ground Station to be considered in the next phases of the Space Rider programme. One possible reduced GSN identified is constituted by Singapore, Kourou, Canberra, Santa Maria, Dongara, and Curacao (Figure 29). It is also remarked that a mobile station in Nueva Guinea, or the inclusion of a fixed station closed to Nueva Guinea, as BIAK, could help monitoring post-separation phases of multiple scenarios (1, 4, 5, 6, 7 and 8).

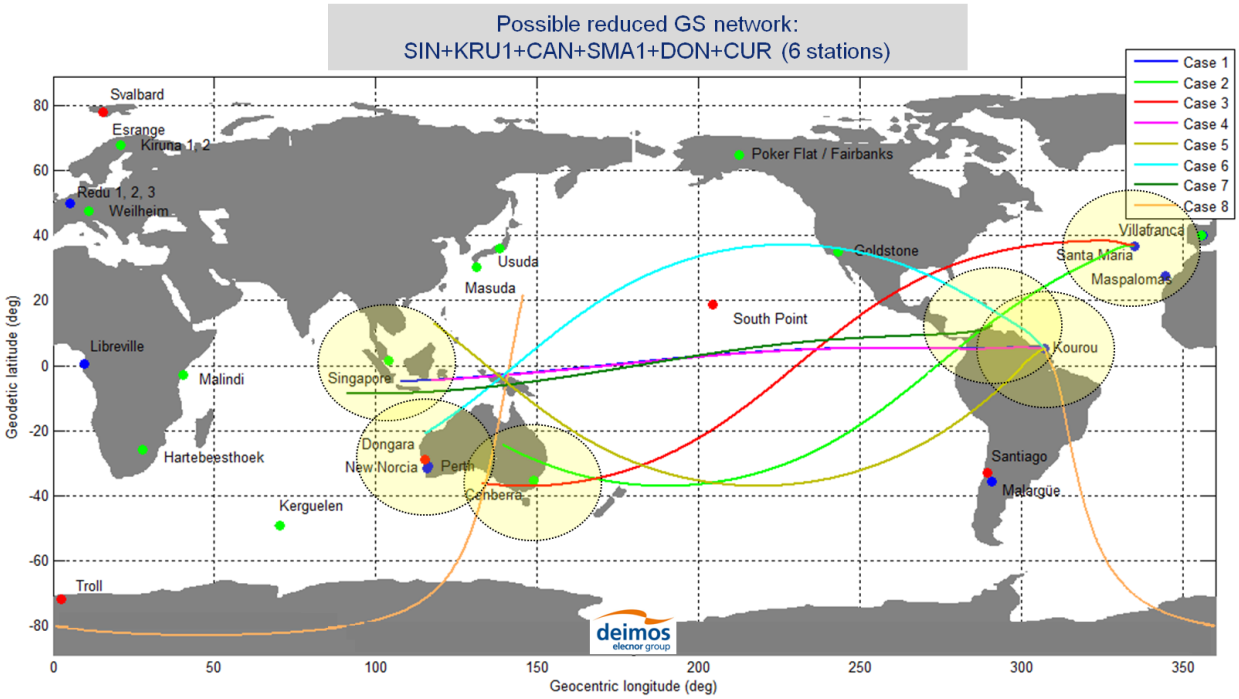

Figure 29: Possible reduced GS network for return phase needs

The link budget is evaluated during the Orbital phase from two different perspectives, aiming to assess if a feasible communication link is possible between SR and the ground stations. On one hand the obtained signal-to-noise ratio (SNR) is calculated at the ground station, which is dependent on the SR transmitter power and antenna gain, the distance from the SR to the GS, atmospheric path losses, and the characteristics of the GS itself. On the other hand, the required SNR that is needed to establish a communication link with the required specifications is calculated. This depends on the required bit rate and admissible error rate, as well as on other characteristics of the communication link. The feasibility of the communication link can then be evaluated by comparing the obtained SNR with the required one, and the difference between the two defines the TM margin. The link budget analysis was performed using the worst-case slant range observed for each elevation angle from the geometric visibility analysis results of the orbital phase. Given the uncertainty of some key parameters, the link budget has been focused on a sensitivity analysis that allows evaluating the effect of several design parameters on the feasibility of establishing the telemetry link. More specifically, the combination of values of Tx power and the GS G/T ratio that result in a positive TM margin have been identified, considering different values for the elevation angle and required data rate (Figure 28). The performed analysis can then be used to support decisions on the design of the communication system and/or selection of ground stations.

10. Conclusions

During the phase B2 of the Space Rider Mission Analysis, multiple activities have been performed to support the trade-offs at system level for the definition of the baseline vehicle configuration and mission solution. The baseline solution feasibility has been assessed, including high fidelity simulations and optimizations of the complete return phase (from deorbiting to touchdown) for multiple mission scenarios, leveraging on consolidated tools and DEIMOS Space Mission Analysis expertise inherited from the IXV mission and the Space Rider phase A. Driving factors that should be tackled in the design consolidation phase of the programme have been identified: consolidation of the system mass budget, further characterization of the aerodynamic properties in supersonic and subsonic and consolidation of the trim strategy, consolidation of the re-entry Guidance to cope with the Space Rider Entry mission needs, consolidation of the descent system design, and full definition of the ground station network.
Considerable variability exists between the different Space Rider mission scenarios in terms of orbit, conditions at the EIP (FPA, velocity), range to be flown during entry and landing sites. These imply the need for a significant missionization process of the Space Rider programme.
Continuous iterations with System activities are currently ongoing as part of the Mission Analysis activities for the phase C of Space Rider, with the overall objective of consolidating the current design toward a successful System Critical Design Review.

Acknowledgments

The work has been performed under the Space Rider programme in Phase B2 and funded by the European Space Agency. The authors wish to thank Thales Alenia Space Italia and ESA teams, for their support to the Space Rider mission analysis activities in Phase B2.

References

[1] Tumino G. et al (2013) "The PRIDE Programme: From the IXV to the ISV", IAC-13, Cape Town, South Africa.
[2] Bonetti D. et al. (2015) "IXV Mission Analysis and Flight Mechanics: from Design to Postflight", 23rd AIDAA, Turin, Italy.
[3] Marini M. et al (2017) "Aeroshape Trade-Off and Aerodynamic Analysis of the Space Rider Vehicle", 7th EUCASS Conference, Milan, Italy.
[4] Bonetti D. et al (2018) "SPACE RIDER: Mission Analysis and Flight Mechanics of the Future European Reusable Space Transportation System", HiSSt Conference, Moscow, Russia.
[5] Haya R. et al (2011) "Flying Qualities Analysis for Re-entry Vehicles: Methodology and Application", AIAA GNC 2011, Portland, USA.
[6] Bastante J.C. et al (2010) "End to end Optimisation of IXV Trajectory via Multiple-Subarc Sequential Gradient Restoration Algorithm", 61st IAC, Prague, Czech Republic.
[7] De Zaiacomo G. et al (2018) "SPACE RIDER: Entry and TAEM GNC of the Future European Reusable Space Transportation System", HiSSt Conference, Moscow, Russia.
[8] Marcos V. et al (2016), "The IXV Guidance, Navigation and Control Subsystem: Development, Verification and Performances", Acta Astronautica, Vol. 124.
[9] Gridded Population of the World (GPW) v4.0 (2015), Socioeconomic Data and Applications Center (SEDAC), http://www.ciesin.org/.

DOI: 10.13009/EUCASS2019-633

[10] Hamlin T.L. et al (2010) "2009 Space Shuttle Probabilistic Risk Assessment Overview", 10th International Probabilistic Safety Assessment and Management Conference, Seattle, USA.